Mon. Not. R. Astron. Soc. **324,** 1087–1101 (2001)

Stellar population gradients in normal and active galaxies

D. Raimann,[1★] T. Storchi-Bergmann,[1★] E. Bica[1★] and D. Alloin[2★]
[1]*Universidade Federal do Rio Grande do Sul, IF, CP15051, Porto Alegre 91501-970, RS, Brazil*
[2]*European Southern Observatory, Casilla 19001, Santiago 19, Chile*

Accepted 2001 February 5. Received 2001 January 16; in original form 2000 November 16

ABSTRACT

We use high signal-to-noise ratio long-slit spectra in the $\lambda\lambda$3500–7000-Å range of three early-type (Hubble type S0) normal, two low-ionization nuclear emission region (LINER) and three Seyfert 2 galaxies to make a comparative study of the variation of the stellar population properties as a function of distance from the nucleus. In order to characterize the stellar population and other continuum sources (e.g. featureless continuum) we have measured equivalent widths (Ws) of six absorption features, continuum colours and their radial variations, and performed spectral population synthesis as a function of distance from the nucleus. The Ws for the normal galaxies are strongest at the nucleus and decrease outwards. The two LINER galaxies show a similar behaviour, but with the nuclear Ws in the blue ($\lambda < 4500$ Å) $\approx$ 10–20 per cent smaller. Both normal galaxies and LINERs present a redder nucleus than their surroundings. The three Seyfert 2 galaxies present the opposite behaviour, with most Ws in the blue being smaller at the nucleus, which is also bluer than outside. By combining the results of the present work with those of a previous study, we conclude that, in a sample of 12 Seyfert 2s of Hubble type S0, 10 ($\approx$80 per cent) present nuclear Ws smaller than those of normal galaxies, while at $\approx$1 kpc from the nucleus this number decreases to 4 ($\approx$30 per cent).

Sampling regions of $\approx$100–200 pc, we conclude that the normal galaxies have nuclear stellar populations dominated by the components with an age of 10 Gyr and metallicity solar or above. The contribution of this component decreases, while that of 1 Gyr increases, with increasing distance from the nucleus. The LINERs present a similar behaviour but have a $\approx$10–20 per cent larger contribution of the 1-Gyr component at the nucleus. For the Seyfert 2 galaxies, there are additional components: in the three cases studied here, there is a significant contribution from a 100-Myr-old population at the nucleus plus featureless continuum in two cases and also of a 3-Myr-old component in Mrk463E. Outside the nucleus, the stellar population is similar to that of normal galaxies in ESO138-G1, but it has an excess of old metal-poor components in NGC7743 and of young components in Mrk463E, when compared with normal galaxies. The reddening of the continuum is lowest in the normal galaxy nuclei [$E(B-V)_i \approx 0.00$] and highest in the Seyfert [$E(B-V)_i \approx 0.20$] nuclei.

Key words: galaxies: active – galaxies: general – galaxies: Seyfert – galaxies: stellar content.

1 INTRODUCTION

Starlight constitutes an important fraction of the optical radiation of nearby low-luminosity active galactic nuclei (AGN), allowing the study of the stellar populations in the nuclear region of the host galaxies, fundamental for understanding the origin of the AGN phenomenon. Methods used in previous works include representing the stellar population of an AGN by the spectrum of the bulge of an elliptical galaxy (Koski 1978), or by means of population synthesis techniques, using a library of stellar spectra plus assumptions about the mass function and star formation history (Keel 1983). Bica (1988) carried out population synthesis using a spectral library of star clusters, which has been used in the study of stellar populations in AGNs by Bonatto, Bica & Alloin (1989), Storchi-Bergmann, Bica & Pastoriza (1990) and Schmitt, Storchi-Bergmann & Cid Fernandes (1999). González Delgado, Leitherer & Heckman (1999) and González Delgado, Heckman & Leitherer (2000) use evolutionary synthesis combined with intermediate age and old stellar population templates for this kind of study.

★E-mail: raimann@if.ufrgs.br (DR); thaisa@if.ufrgs.br (TS-B); bica@if.ufrgs.br (EB); dalloin@eso.org (DA)

Although, in the past, it has been assumed that Seyfert nuclei are mostly found in early-type galaxies with the old stellar population typical of elliptical galaxies, recent studies have shown that, in many Seyfert 2 galaxies, stars younger than 100 Myr are found in the vicinity of the nucleus in larger proportions than in elliptical galaxies (Cid-Fernandes, Storchi-Bergmann & Schmitt 1998; Storchi-Bergmann, Cid-Fernandes & Schmitt 1998; Schmitt et al. 1999; Storchi-Bergmann et al. 2000). Detailed *Hubble Space Telescope* (*HST*) observations in the UV of four Seyfert 2 nuclei have revealed the presence of compact, reddened and powerful starbursts responsible for most of the blue light in these galaxies (Heckman et al. 1997; González Delgado et al. 1998). Young stellar populations have been found also in the nuclear regions of nearby radio galaxies (e.g. Aretxaga et al. 2001).

The relevant questions in the study of the stellar population of AGNs are: is there a connection between nuclear activity and star formation? What are the ages and metallicities of the stars in and around AGNs? What fraction of Seyfert galaxies exhibits signs of recent star formation? Do AGNs evolve along with their neighbouring stars? In order to answer these questions, it is necessary to determine the age and metallicity of the stellar population of a statistically significant sample of AGNs, as well as those of a comparison sample of normal galaxies, matched in Hubble type, luminosity and distance to the Seyfert hosts. This work is a step towards such a goal. We have collected long-slit spectra on eight early-type galaxies comprising normal, low-ionization nuclear emission region (LINER) and Seyfert 2 galaxies to obtain the stellar population characteristics not only at the nucleus but up to 10–20 arcsec from it, corresponding to ≈2 kpc from the galaxy, with a typical spatial resolution of 100–200 pc.

We first investigate the dilution of the nuclear absorption lines by a featureless continuum (FC) or young stellar population, through the study of the radial variations of the equivalent widths, and subsequently we perform spectral synthesis at the nucleus and along the inner region of the galaxy. In order to test the robustness of the method in discriminating between the different components of the spectra, we also present the results of some tests performed on simulated composite spectra.

This paper is organized as follows. In Section 2 we present the sample galaxies and the observations. In Section 3 we discuss the spatial variation of the equivalent widths and continuum. In Section 4 we discuss the method of spectral synthesis. We present the stellar population gradient results in Section 5 and, in Section 6, the conclusions of this work.

2 OBSERVATIONS

The sample comprises three Seyfert 2, two LINER and three normal galaxies. Except for Mrk463E, they are nearby objects with radial velocities <3000 km s^{-1}. In Table 1 we list the activity type, morphology, radial velocity, total apparent blue magnitude, foreground galactic $E(B-V)_{\rm G}$ values from Burstein & Heiles (1982, derived from H I and galaxy counts) and those by Schlegel, Finkbeiner & Davis (1998, derived from dust infrared emission at 100 μm). The latter two values agree within the observational errors for the present sample. The data were extracted from the NASA/IPAC Extragalactic Database (NED).

Long-slit spectra of these galaxies have been obtained using the Cassegrain spectrograph with the 4-m Blanco telescope of Cerro Tololo Interamerican Observatory in 1997 May and September. The long-slit spectra cover the spectral range 3500–7000 Å, at a resolution of ≈4 Å. Each pixel at the detector corresponds to 0.5 arcsec in the sky. A slit width corresponding to 1.5 arcsec on the sky was oriented along the parallactic angle except for ESO138-G1 on which it was oriented at 36° from it, still allowing all the optical light to fall within the slit.

A log of the observations is presented in Table 2, where we list the date, exposure time, slit position angle (PA), air mass during the observations and spatial scale in pc arcsec^{-1} (for $H_0 = 75$ km s^{-1} Mpc^{-1}).

Table 1. The sample.

Name	Activity	Morphology	V (km s^{-1})	B (mag)	$E(B-V)_{\rm G(H\,I)}$	$E(B-V)_{\rm G(100\,\mu m)}$
NGC6684	Normal	(L)SB(r)0+	847	11.31	0.053	0.067
NGC6861	Normal	SA(s)0−	2819	12.12	0.036	0.054
NGC7049	Normal	SA(s)0	2231	11.72	0.007	0.054
IC1459	LINER	E3	1691	10.97	0.010	0.016
NGC1052	LINER	E4	1470	12.08	0.015	0.027
NGC7743	Seyfert 2	(R)SB(s)0+	1710	12.38	0.041	0.070
ESO138-G1	Seyfert 2	E-S0	2470	14.31	0.225	0.200
Mrk463E	Seyfert 2		14990	17.25	0.005	0.030

Table 2. Log of observations.

Name	Date	Exp. Time (s)	PA [°]	Air mass	Scale (pc arcsec^{-1})
NGC6684	1997 May 1	1800	155	1.26	55
NGC6861	1997 May 1	1800	125	1.14	182
NGC7049	1997 May 1	1800	116	1.19	144
IC1459	1997 September 24	1800	6	1.00	109
NGC1052	1997 September 24	1800	182	1.08	95
NGC7743	1997 September 24	1800	177	1.30	110
ESO138-G1	1997 May 1	1800	1	1.15	160
Mrk463E	1997 May 2	1800	162	1.55	968

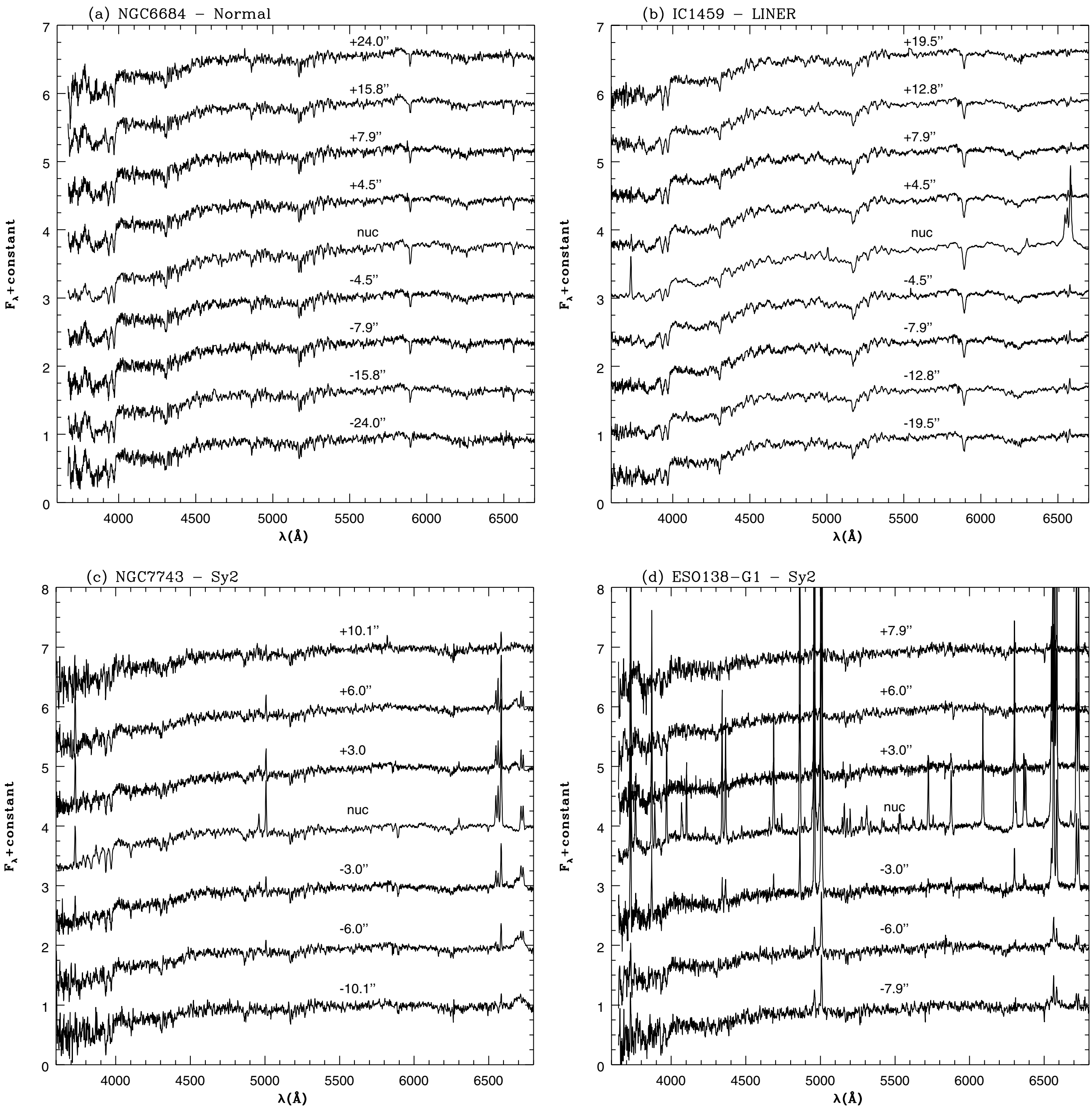

Figure 1. Examples of the spatially resolved spectra of four of the sample galaxies. The angular distances from the nuclei are indicated. The spectra are normalized at 5870 Å and shifted vertically to facilitate comparison. Residual telluric emission lines have been removed.

Reduction and sky subtraction were performed using standard techniques in IRAF. One-dimensional spectra were extracted in windows of 1.5 arcsec in the bright nuclear regions (≈100–200 pc) and progressively larger windows towards the fainter outer regions. The spectra were dereddened according to foreground galactic $E(B-V)_{\mathrm{G}(100\,\mu\mathrm{m})}$. The spatial coverage ranged between 3 (for Mrk463E) and 34 arcsec (NGC6684) from the nucleus. The signal-to-noise ratio at 5900 Å ranged between 10 and 100. Fig. 1 shows representative spectra of the sample galaxies for several positions along the slit.

3 RADIAL VARIATION OF THE EQUIVALENT WIDTHS AND CONTINUUM COLOURS

The variation of the equivalent widths (Ws) of absorption lines and the monochromatic continuum colours as a function of distance from the nucleus allows the study of stellar population gradients in the galaxy and, in particular, allows us to detect if there is any dilution by an FC or a young stellar population at the nucleus or in the circumnuclear region (Cid-Fernandes et al. 1998).

In order to study the run of the stellar absorption features with distance from the nucleus, we determined a pseudocontinuum at selected pivotpoints and measured the Ws of six absorption features, integrating the flux within each window between the pseudocontinuum and the spectrum for each extraction window.

The pivot points for the continuum are 3660, 3780, 4020, 4510, 4630, 5313, 5870 and 6080 Å and the absorption features for which we measured the Ws are: W_{wlb} (a blend of weak lines in the near-UV, within the spectral window λλ3810–3822 Å), H9 (a blend of absorption lines which includes H9, λλ3822–3858 Å), Ca II K (λλ3908–3952 Å), Ca II H + Hϵ (λλ3952–3988 Å), CN-band (λλ4150–4214 Å), G-band (λλ4284–4318 Å), Mg I+MgH (λλ5156–5196 Å) and Na I (λλ5880–5914 Å).

Ws and continuum definitions are based on Bica & Alloin (1986a), Bica (1988) and Bica, Alloin & Schmitt (1994, hereafter BAS94). The use of the same set of pivot points and wavelength windows allows a detailed quantitative analysis of the stellar population via synthesis techniques using the spectral library of star clusters of Bica & Alloin (1986a) and Bica (1988).

Comparing the nuclear Ws with those at 3 arcsec from the

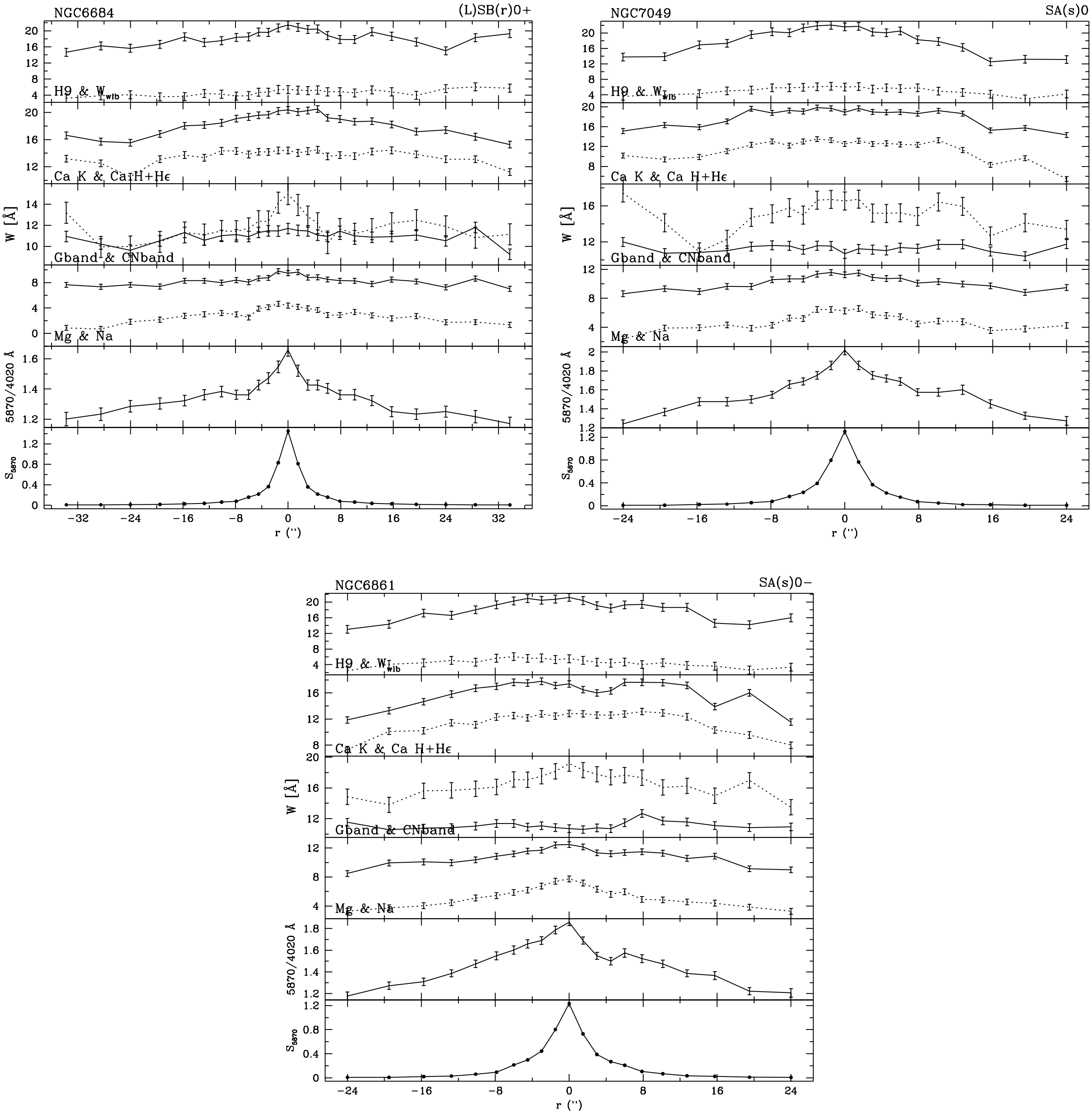

Figure 2. Radial variations of the equivalent widths (Ws), colours and surface brightness for the three normal galaxies. The first panel shows W_{H9} (solid line) and W_{wlb} (dotted), the second shows the $W_{Ca\,II K}$ (solid) and $W_{Ca\,II H+H\epsilon}$ (dotted), the third, the $W_{G\text{-band}}$ (solid) and $W_{CN\text{-band}}$ (dotted), and the fourth panel shows $W_{Mg\,I+MgH}$ (solid) and $W_{Na\,I}$ (dotted). The fifth panel shows the continuum colour $C_{5870/4020}$ (solid, left-hand scale). The sixth panel shows the run of the surface brightness at 5870 Å (in units of 10^{-15} erg cm^{-2} s^{-1} Å^{-1} arcsec^{-2}) along the slit. The vertical bars are the errors of the measurements.

nucleus, we can estimate the fraction of the continuum associated with a FC component or a young population under the assumption that the underlying stellar population at the nucleus is the same as outside. The dilution factor [$f(\lambda)$] that gives the FC/young fraction of the total continuum spectrum at the wavelength of an absorption line is estimated by

$$f(\lambda) = \frac{W_{\mathrm{off-nuc}} - W_{\mathrm{nuc}}}{W_{\mathrm{off-nuc}}}, \tag{1}$$

where W_{nuc} and $W_{\mathrm{off-nuc}}$ are the Ws at the nucleus and outside, respectively (Cid-Fernandes et al. 1998).

In Figs 2, 3 and 4 we present the above Ws, continuum colour F_{5870}/F_{4020} (hereafter $C_{5870/4020}$) and surface brightness as a function of the angular distance from the nucleus for the normal, LINER and Seyfert 2 galaxies, respectively.

The normal galaxies (NGC 6684, 6861 and 7049) show a redder nucleus, with typical colours $1.6 < C_{5870/4020} < 2.0$ to 1.3–1.6 at ≈1 kpc from the nucleus. The Ws are larger at the nucleus than outside. Typical nuclear values are: $W_{\mathrm{H9}} = 20$Å, $W_{\mathrm{wlb}} = 6$Å, $18 < W_{\mathrm{Ca\,II K}} < 20$ Å, $12 < W_{\mathrm{Ca\,II H+H\epsilon}} < 14$ Å, $W_{\mathrm{G-band}} = 11$ Å, $17 < W_{\mathrm{CN-band}} < 19$ Å, $9 < W_{\mathrm{Mg\,I+MgH}} < 12$ Å and $4 < W_{\mathrm{Na\,I}} <$ 6 Å, and decreasing typically by ≈2 Å at ≈1 kpc from the nucleus.

The Ws and continuum colours (Cs) of the LINER galaxies show a similar radial behaviour to those of normal galaxies, but exhibit somewhat lower values for W_{H9}, W_{wlb}, $W_{\mathrm{Ca\,II K}}$ and $W_{\mathrm{Ca\,II H+H\epsilon}}$ at the nucleus, more noticeable in NGC1052 (2–4 Å smaller, in this case). The nuclear colours are as red as those of the reddest normal galaxy. Regarding dilution of the nuclear Ws, it was detected in the two LINERs only for Ca II H+Hϵ: 10 ± 1 per cent for IC1459 and 24 ± 1 per cent for NGC1052. As such dilution was not detected in the other Ws in the blue, it is most probably a result of a weak Hϵ emission line.

The behaviour of the Seyfert 2 Ws and colours is more complex and very different from the above. Most nuclear colours are bluer and most Ws smaller than those of normal galaxies or LINERs. We thus discuss the results for each Seyfert 2 galaxy separately.

The NGC7743 nuclear colour $C_{5870/4020}$ is bluer than in the neighbouring regions. At ≈1 kpc from the nucleus, this value is similar to that of normal galaxies. The nuclear Ws are 50 per cent smaller than those in normal galaxies in the blue to 30 per cent smaller in the cases of Mg I+MgH and Na I. At 1 kpc from the nucleus, the Ws look more similar to those of normal galaxies, except for W_{H9} and W_{CN}, which are still 30–40 per cent smaller. Only $W_{\mathrm{Ca\,II K}}$ and $W_{\mathrm{CN\text{-}band}}$ show nuclear dilutions of 33 ± 3 and 17 ± 2 per cent, respectively.

In the case of ESO138-G1, $C_{5870/4020}$ is bluer at the nucleus than outside and it is bluer than normal galaxies. This colour get redder further from the nucleus, reaching values at ≈2 kpc which are ≈30 per cent bluer than normal galaxies. All nuclear Ws are smaller than extranuclear ones, corresponding to dilutions of 59 ± 1 per cent in H9, 55 ± 1 per cent in Ca II K, 53 ± 2 per cent in the CN-band and 54 ± 3 per cent in the G-band. The Ca II H+Hϵ and Mg I+MgH windows are filled by emission. At ≈1 kpc from the nucleus most Ws are similar to those of normal galaxies, except for the CN-band, Mg I+MgH and Na I, which are still ≈30 per cent smaller.

Mrk463E is a much more distant galaxy with a scale ≈6 times larger than the previous cases, used here as a test of the method for more distant Seyferts. The spectra are dominated by line-emission, and the Balmer continuum accounts for ≈7 per cent of the flux at $\lambda5870$ Å, 8 per cent at $\lambda3660$ Å and 30 per cent at $\lambda < 3646$ Å. The nuclear $C_{5870/4020}$ is bluer than is in the case in normal galaxies, with the extranuclear values somewhat bluer than the nuclear one and still bluer than those of normal galaxies at similar distance from the nucleus. Dilution of the nuclear Ws are observed in Ca II K and G-band with dilution factors of 78 ± 2 per cent and 69 ± 6 per cent, respectively. H9, Ca II H+Hϵ, Mg I+MgH and Na I are filled with emission. Outside the nucleus the blue Ws (W_{H9}, $W_{\mathrm{Ca\,II K}}$, $W_{\mathrm{G\text{-}band}}$ and W_{CN}) are still strongly diluted when compared with those of normal galaxies at similar distances from the nucleus.

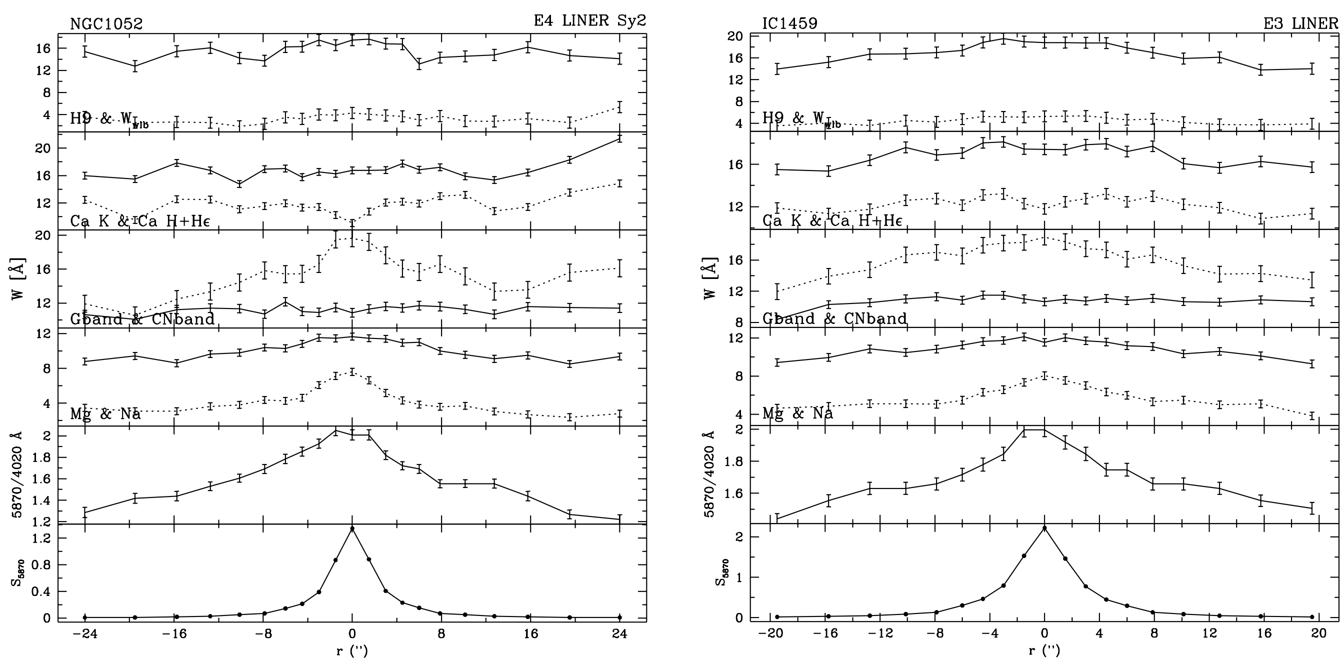

Figure 3. LINERs: as in Fig. 2.

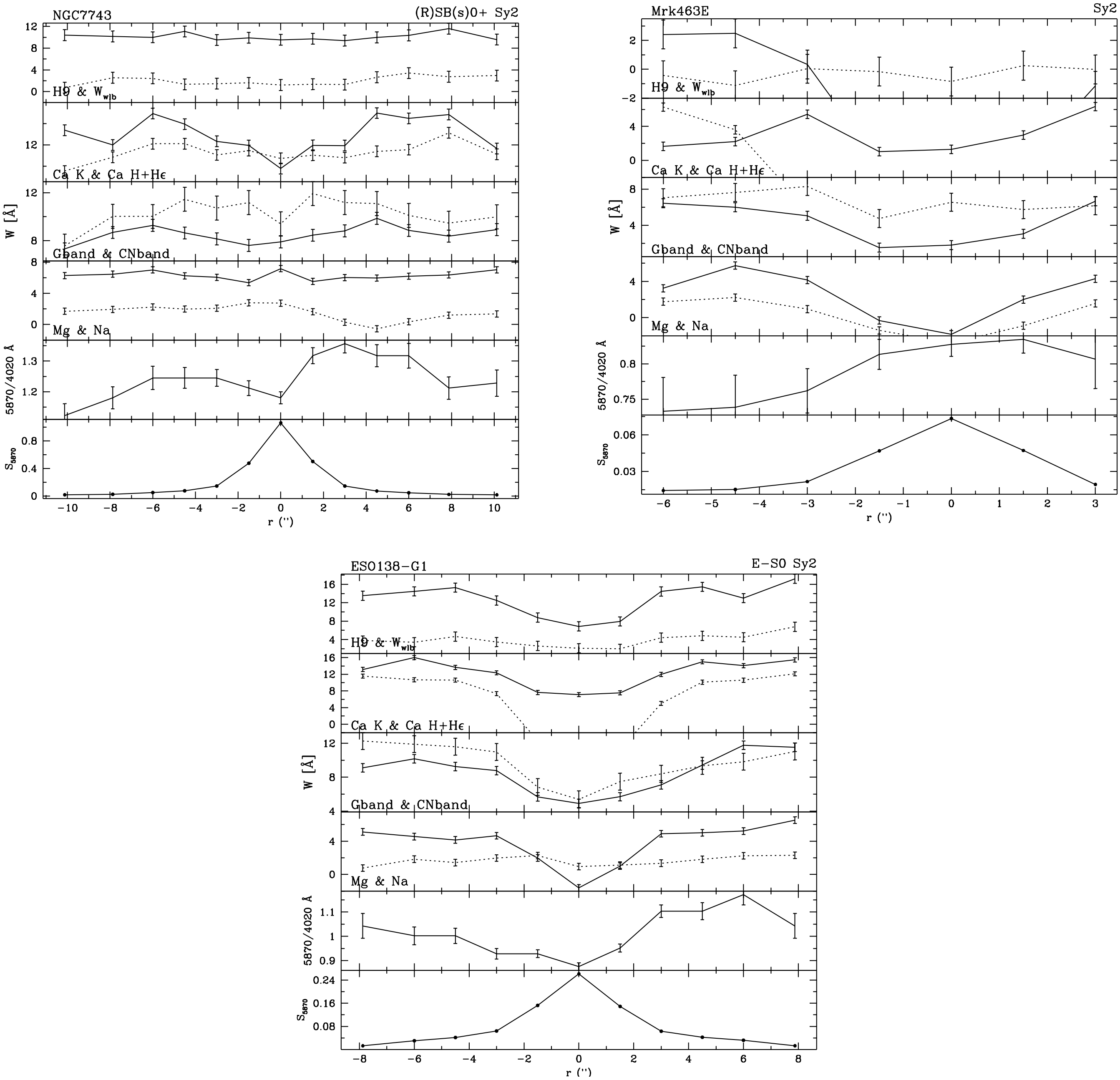

Figure 4. Seyferts: as in Fig. 2.

Results for Seyfert 2s can be compared with those of the S0 Seyfert 2s from the larger sample of Cid Fernandes et al. (1998). The nuclear $W_{Ca\,II\,K}$ values of seven out of nine S0 Seyfert 2s studied in that work are smaller than ≈15Å, thus diluted relative to the nuclear values of the normal and LINER galaxies. At ≈1 kpc from the nucleus, the values tend to be similar to those of normal galaxies and LINERs, except in three cases in which they are smaller. These results are thus similar to those in the present paper. Putting together the two samples, we can claim that in 10/12 (≈80 per cent) of S0 Seyfert 2s there is dilution of the nuclear Ws when compared with normal and LINER galaxies. At 1 kpc, only 4/12 (≈30 per cent) still present significant (>30 per cent) dilution of their blue Ws when compared with the values in normal galaxies at the same distance from the nucleus.

4 THE METHOD OF SPECTRAL SYNTHESIS

The spectral synthesis at the nucleus and outside was performed using Bica's (1988) code, modified by Schmitt, Bica & Pastoriza (1996) to include continuum ratios and internal reddening in the search for solutions. With this method we reproduce the observed Ws and continuum ratios (Cs) using a base of star clusters with different ages and metallicities (Bica & Alloin 1986a). We use 12 components representing the age–metallicity plane plus an extra component representing a cannonical AGN continuum $F_\nu \propto \nu^{-1.5}$. These components are listed in Table 3. The FC component was introduced in the synthesis by Schmitt et al. (1999) for the spectral synthesis of the nuclear region of Seyfert 2 and radio galaxies.

The code adds different proportions in flux at λ5870 Å of the base elements in steps of 5 per cent, constructing all possible combinations of the elements, and compares the Ws and Cs of these combinations with the observed values. A combination is an acceptable solution when all observed and synthesized values agree within an error window. These windows are typically of 1–2 Å for Ws and 0.05–0.10 for Cs, which are of the order of the observational errors. The internal reddening $E(B-V)_i$ is tested in the 0–0.50 range, with a step of 0.02.

Table 3. Base elements in the age × metallicity plane.

3 Myr	10 Myr	100 Myr	1 Gyr	10 Gyr	$[Z/Z_\odot]$
	10	8	5	1	+0.6
12	11	9	6	2	0.0
			7	3	−1.0
				4	−2.0

Plus the 13th component, FC of the form $F_\nu \propto \nu^{-1.5}$.

More than one solution can represent the observed data because spectral synthesis is a degenerate problem. The final solution is the weighted average of all solutions, for the $E(B-V)_i$ value that gives the smallest χ^2, where

$$\chi^2 = \sum_{i=1}^{6} (W_{\rm oi} - W_{\rm si})^2/\sigma_{wi}^2 + \sum_{j=1}^{4} (C_{\rm oj} - C_{\rm sj})^2/\sigma_{cj}^2 \qquad (2)$$

and W_{oi} and W_{si} are the observed and synthesized Ws, respectively,

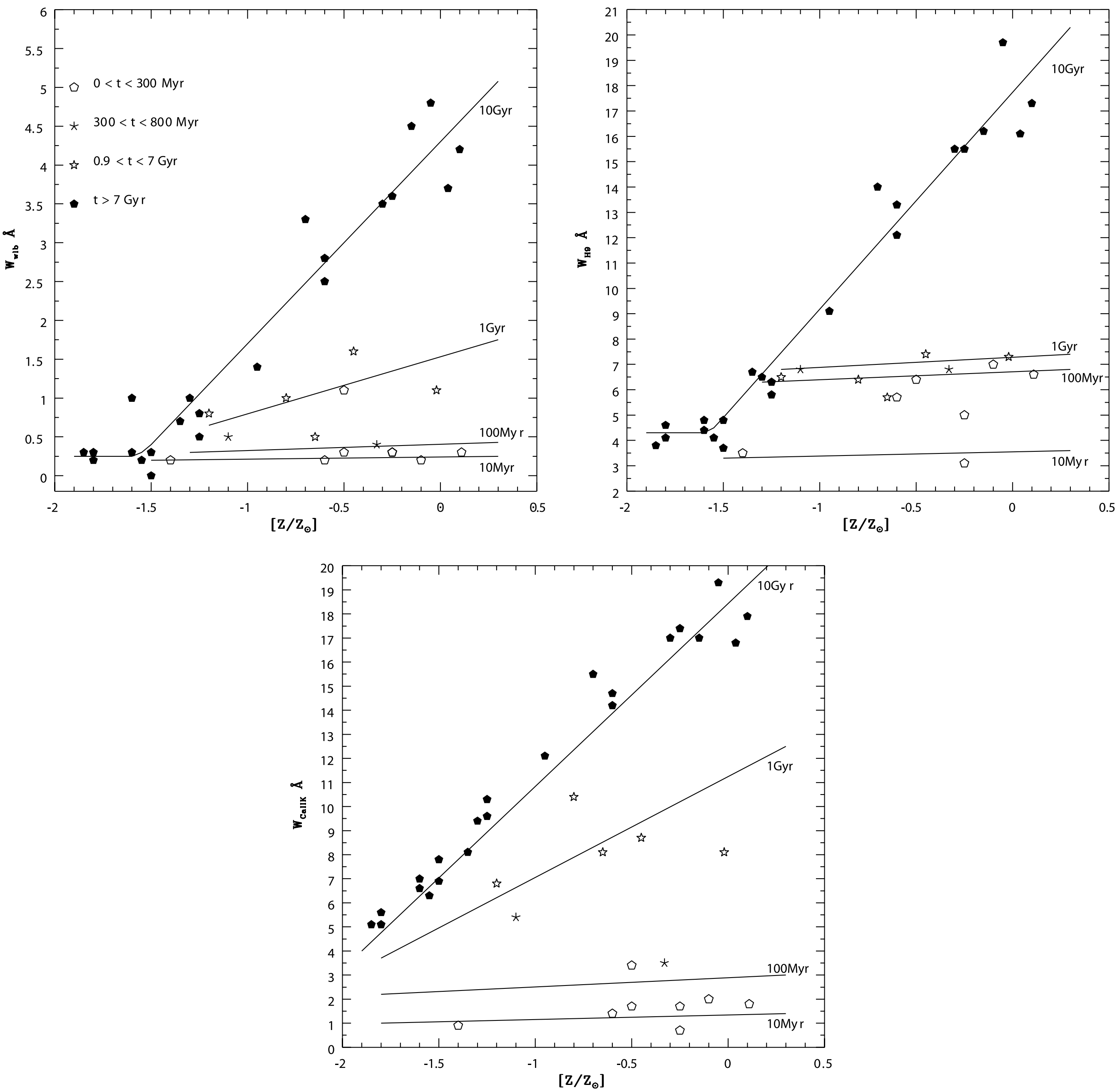

Figure 5. Equivalent widths $W_{\rm wlb}$, $W_{\rm H9}$ and $W_{\rm Ca\,II K}$ as a function of metallicity for star clusters of different ages (BAS94). The different symbols represent the age groups identified in the first panel.

C_{oj} and C_{sj} are the observed and synthesized Cs and σ_{wi} and σ_{cj} are the measurement errors of the Ws and Cs.

The results of the synthesis are presented as proportions of the flux contributed by each component at λ5870 Å and the internal reddening $E(B-V)_i$ of the galaxy.

To synthesize the data of this work we have used the Cs λ3660/5870, λ4020/5870, λ4510/5870 and λ6630/5870, and the Ws W_{wlb}, W_{H9}, $W_{Ca\,II K}$, $W_{CN\text{-band}}$, $W_{G\text{-band}}$ and $W_{Mg\,I+MgH}$. The adopted typical errors of Ws (σ_{wi}) were 0.5Å for W_{wlb}, W_{H9}, $W_{Ca\,II K}$ and $W_{G\text{-band}}$, 0.4Å for $W_{Mg\,I+MgH}$, and 1.0Å for $W_{CN\text{-band}}$ (Cid Fernandes et al. 1998).

Table 4. Equivalent widths W_{wlb}, W_{H9} and $W_{Ca\,II K}$.

Age	[Z/Z$_\odot$]	W_{wlb}	W_{H9}	$W_{Ca\,II K}$
10 Gyr	+0.6	5.9	22.8	22.9
10 Gyr	0.0	4.3	17.7	18.6
10 Gyr	−1.0	1.7	9.1	11.3
10 Gyr	−2.0	0.3	4.3	4.0
1 Gyr	+0.6	1.4	7.5	10.4
1 Gyr	0.0	1.1	7.3	8.8
1 Gyr	−1.0	0.7	7.0	6.0
100 Myr	+0.6	0.4	6.9	3.2
100 Myr	0.0	0.4	6.8	2.9
10 Myr	+0.6	0.3	3.6	1.5
10 Myr	0.0	0.2	3.5	1.3
3 Myr	0.0	0.0	0.0	0.0
FC	–	0.0	0.0	0.0

4.1 New features in the synthesis

Relative to previous works, here we include two new absorption features in the synthesis: W_{wlb} and W_{H9}. We use also the new values of $W_{Ca\,II K}$ from the study of near-ultraviolet integrated star cluster spectra by BAS94. We include these features since they add new constraints for intermediate age and young stellar populations and the FC component in AGNs (Storchi-Bergmann et al. 2000).

In order to obtain reference values for the new features in the age × metallicity plane, we use the measurements of W_{H9}, W_{wlb}, $W_{Ca\,II K}$ for star clusters from BAS94. These measurements are plotted in Fig. 5. Following Bica & Alloin (1986a), we have used the known ages and metallicities of the clusters to find the loci for the 10 and 100 Myr, 1 and 10 Gyr ages in the planes W × [Z/Z$_\odot$]. We fitted straight lines to the 10-Gyr and $t < 100$-Myr samples, which are well populated. Subsequently, we interpolated straight lines corresponding to the other age bins with the constraint that they should cover the loci of the few clusters available with a corresponding age. From these 'equal ages' lines, we derive the Ws values for the base elements as a function of age and metallicity that are listed in Table 4.

For populations younger than $t < 100$ Myr (and $t < 1$ Gyr in the case of H9) the Ws of the features in Fig. 5 are basically degenerate. Nevertheless, the corresponding continuum distributions – which are employed together with the Ws in the present work – are non-degenerate (Bica & Alloin 1986a,b; BAS94), therefore allowing us to make the age determinations.

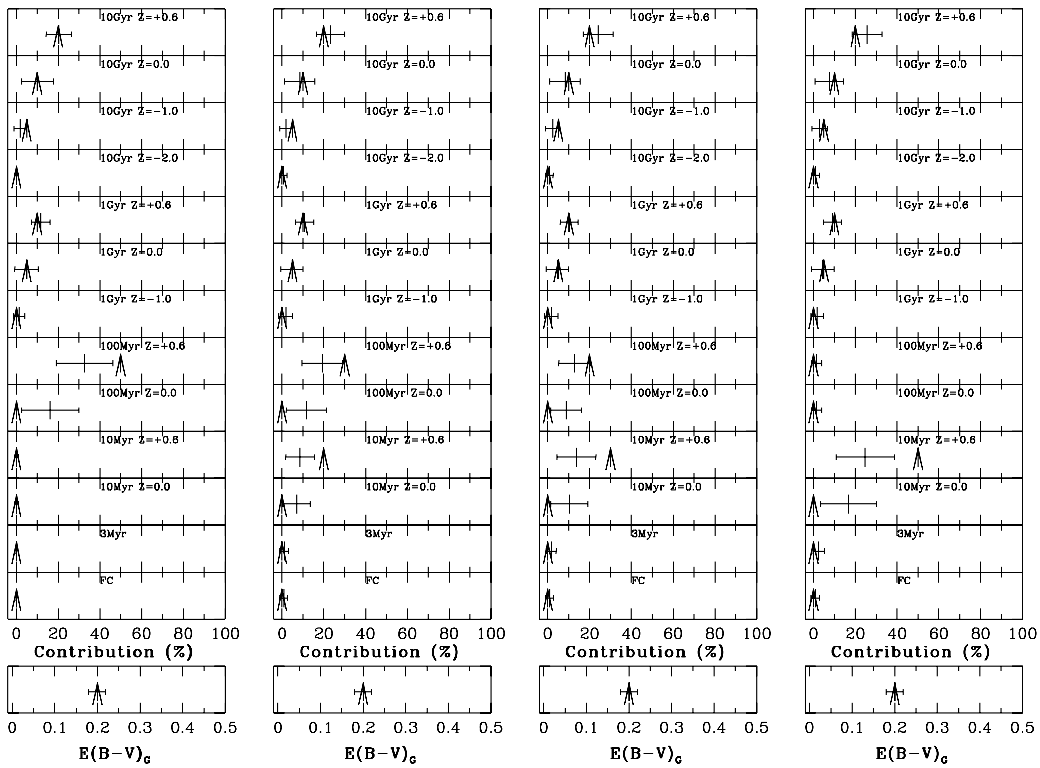

Figure 6. Results for a simulated composite spectrum. The panels, from top to bottom, each correspond to a component of the base, with age and metallicity identified in each panel. The arrow shows the percentage of the flux contribution of each component to the total light at λ5870 Å, while the vertical line indicates the value recovered from the synthesis. The horizontal bars correspond to the standard deviation of the mean. The stellar population has an old component (10 Gyr) contributing 35 per cent of flux at λ5870 Å, a 1-Gyr population contributing 15 per cent and the remaining 50 per cent of the flux is split between 100 and 10 Myr. This is an ideal case, in which the error windows are 0.2 Å for Ws and 0.02 for Cs. Most components are recovered in the synthesis but there is a degeneracy in metallicity among young components.

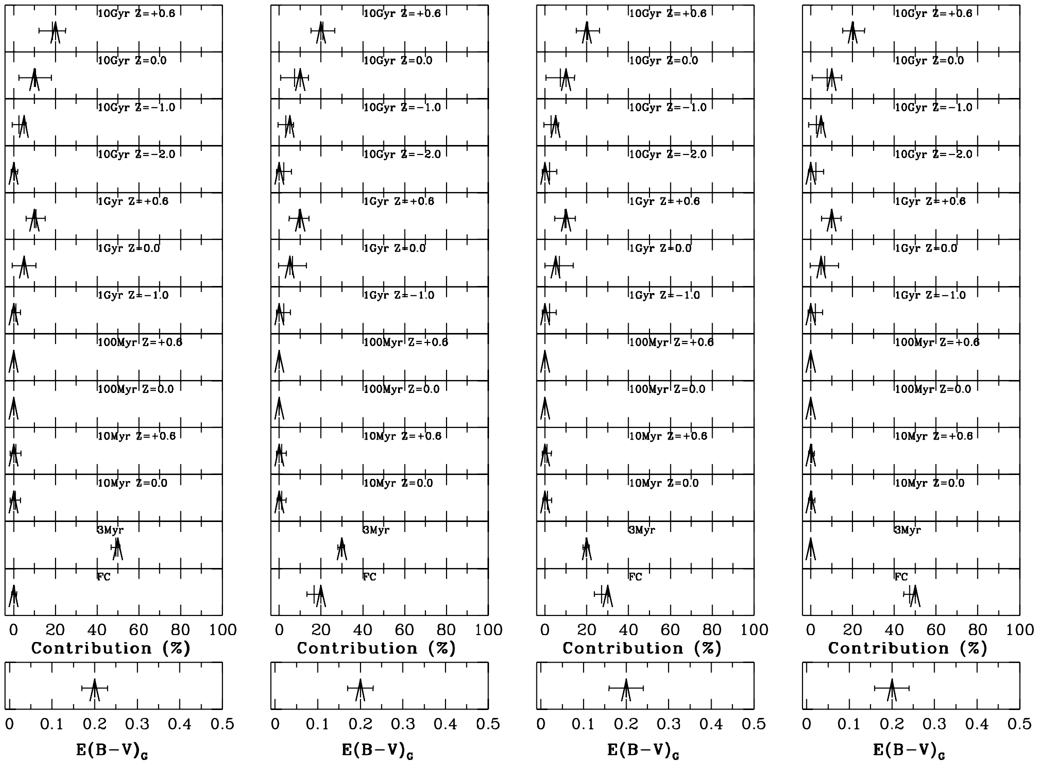

Figure 7. Same as Fig. 6 for simulated composite spectrum where 50 per cent of the flux at λ5870 Å is split between 3 Myr and FC. The components are recovered in the synthesis.

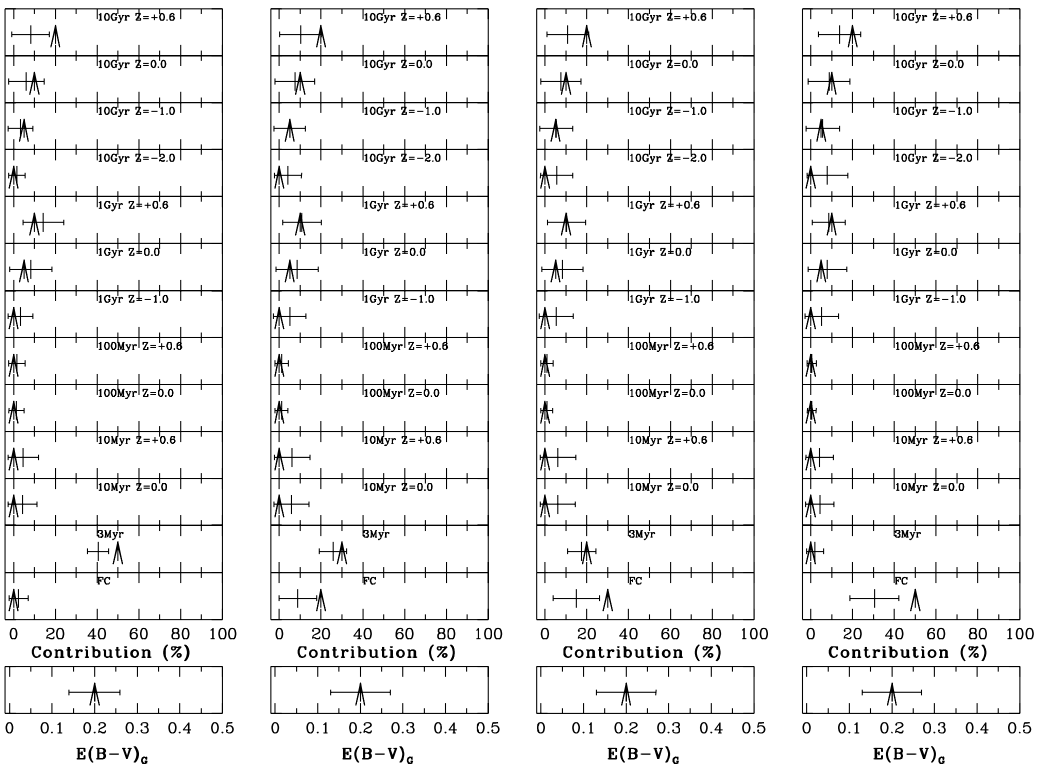

Figure 8. Same as Fig. 6 for simulated composite spectrum where 50 per cent of the flux at λ5870 Å is split between 3 Myr and FC. The error windows are 3 Å for Ws and 0.15 for Cs. It is not possible to recover the FC, as part of its contribution appears under the 10-Myr component and/or under the low-metallicity components of 1 and 10 Gyr.

4.2 Tests of the method in the current spectral range

In order to analyse the behaviour of the solutions in the syntheses of the galaxy spectra, and to determine the conditions (errors, stellar population distributions, signal-to-noise ratio, spectral range) under which the method gives the best results, we have performed a set of tests with simulated composite spectra.

Since our interest is in the stellar population of AGNs, and in particular, to distinguish intermediate age, young stellar populations and FC in AGNs, we have constructed for the tests composite spectra with an old population (10 Gyr) contributing 35 per cent of the flux at $\lambda5870$ Å, a 1-Gyr population contributing 15 per cent and the remaining 50 per cent originating from various proportions of components with ages 100, 10 and 3 Myr, as well as FC. The adopted internal reddening is $E(B-V)_i = 0.20$.

We show in Fig. 6 the result of a test in which 50 per cent of the flux at $\lambda5870$ Å is split between the 100- and 10-Myr age components. In this ideal case, we have used small error windows of 0.2 Å for Ws and 0.02 for Cs. It can be seen that the two age components are recovered in the synthesis, but that there is a

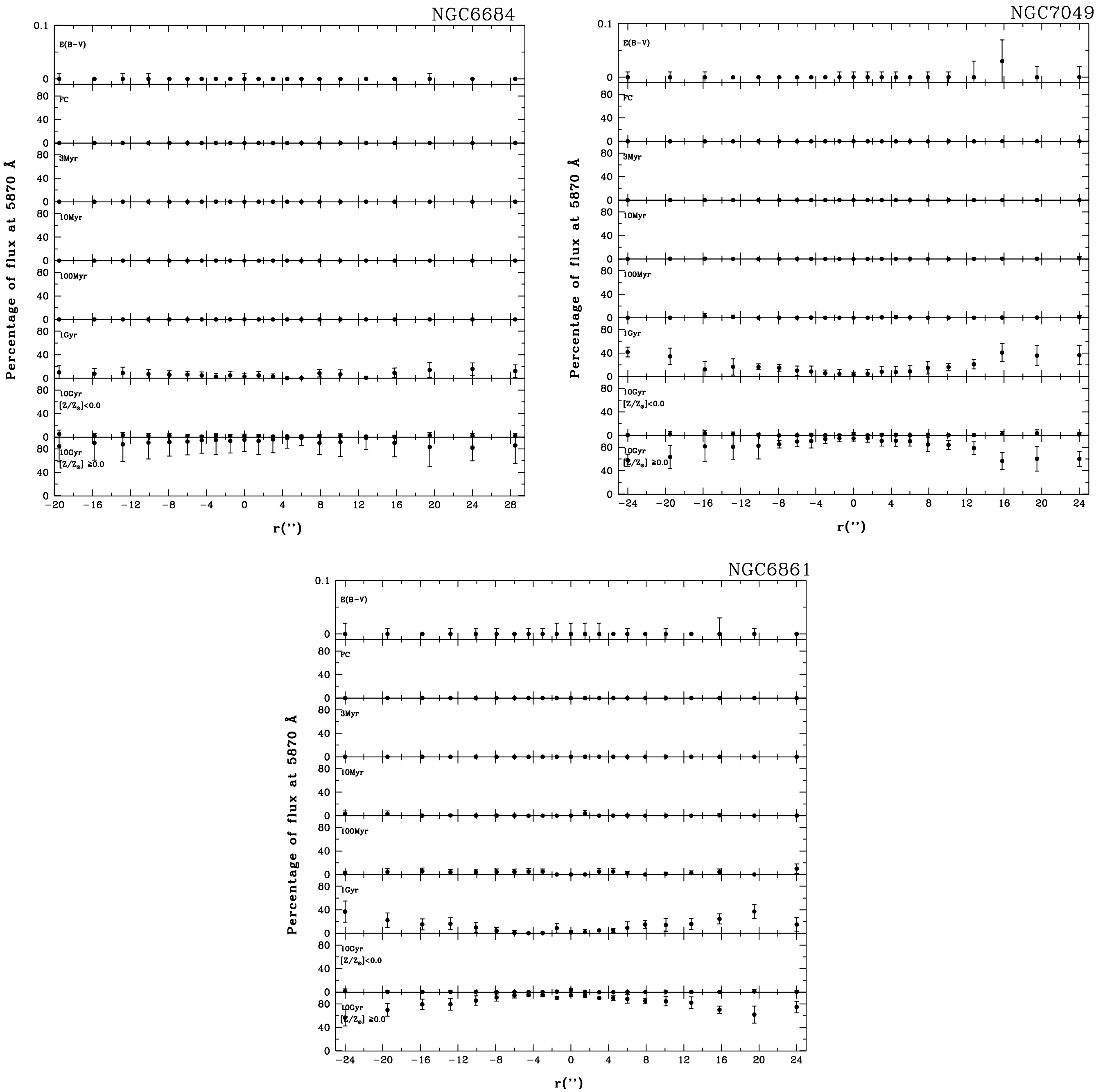

Figure 9. Results of stellar population synthesis using a base of star clusters plus a power-law component $F_\nu \propto \nu^{-1.5}$ for three normal galaxies. These results show percentage of the contribution to the flux at 5780 Å from different age and metallicity components as a function of distance from the nucleus. The panels show, from bottom to top, the contribution from: the sum of old metal-rich (10 Gyr) components; the sum of old metal-poor components; the sum of the three 1-Gyr components; the sum of two 100-Myr components; the sum of the two 10-Myr components; the 3-Myr component; and finally FC ($F_\nu \propto \nu^{-1.5}$). The top panel shows the internal reddening $E(B-V)_i$ obtained from the synthesis. The vertical bars are the standard deviation of the results.

degeneracy in metallicity. Similar tests were performed for 50 per cent of the flux at λ5870 Å distributed among (a) 100 and 3 Myr, (b) 100 Myr and FC, (c) 10 and 3 Myr, (d) 10 Myr and FC and (e) 3 Myr and FC. The latter is illustred in Fig. 7. The results were similar to those of Fig. 6: in all tests it was possible to recover the different age components, as well as the FC, but in the cases with more than one metallicity component, it was not possible to discriminate them; the synthesis usually distributes the flux between $[Z/Z_\odot] = 0.0$ and $+0.6$. The metallicity degeneracy amoung young components can be avoided by the inclusion of the near-infrared range where the Ca II triplet is sensitive to metallicity at essentially all ages (Bica & Alloin 1987; Bica 1988). Also, metal lines in the UV can alleviate this degeneracy (Bonatto et al. 1998).

Another test is shown in Fig. 8, in which we have used larger error windows of ≈3 Å for Ws and 0.15 for Cs, somewhat in excess of those in typical observations. We show the case of 50 per cent of the flux at λ5870 Å split between the 3-Myr and FC components. It is not possible to recover completely the FC when this component is present: approximately half of its contribution appears in the synthesis under 10 Myr components and half under the low-metallicity components of ages 10 Gyr ($[Z/Z_\odot] = -2.0$) and 1 Gyr ($[Z/Z_\odot] = -1.0$). In addition, there is also a decrease in the contribution of the 10-Gyr-old metal-rich ($[Z/Z_\odot] = +0.6$) component.

We have also performed some tests changing the parameters Ws and Cs used in the synthesis. Using only the Ws and Cs of the work by Schmitt et al. (1999), the degeneracy problem is more pronounced. Some improvement is obtained by adding a continuum point in the near-UV, at λ3290 Å.

In summary, the tests show that the synthesis in the current spectral domain gives robust results in terms of age, discriminating well between the different components. On the other hand, it gives degerate results in terms of metallicity within the 10- and 100-Myr age bins. For high signal-to-noise ratios (>50), it is possible to recover an FC, but if this is not the case (signal-to-noise ratio ≤10), there is also degeneracy between FC, the 10-Myr age component and the low-metallicity 10- and 1-Gyr components.

5 STELLAR POPULATION GRADIENTS

We now present the results of the spectral synthesis as a function of distance from the nucleus using the method described in Section 4.

The synthesis results for normal galaxies are illustrated in Fig. 9. The component with age 10 Gyr and high metallicity (solar metallicity and above – hereafter old metal-rich) is dominant. At the nucleus it contributes about 90–95 per cent of the flux at λ5870 Å, decreasing outwards to about 80–85 per cent at 1 kpc and ≈60 per cent at 3 kpc. The 1-Gyr component contributes about 5–10 per cent of flux at the nucleus and about 40 per cent in the outer regions. The components younger than 1 Gyr and the FC do not contribute significantly. The internal reddening $E(B-V)_i$ is ≈0.00 throughout most of the observed regions.

The behaviour of the stellar populations of the LINER galaxies (Fig. 10) is similar to that of normal galaxies, although the old metal-rich component at the nucleus is not as strong and the 1-Gyr component is stronger at the nucleus of the LINERs than in the normal galaxies. At the nucleus, the old metal-rich component contributes 80–85 per cent of the flux, while the 1-Gyr component contributes the remaining 15–20 per cent. At 1 kpc, these proportions are ≈70–75 per cent and 25–30 per cent, respectively. The nuclear reddening values are also larger than in normal galaxies, being $E(B-V)_i = 0.13$ for NGC1052 and $E(B-V)_i = 0.05$ for IC1459.

For the Seyfert 2s (Fig. 11) there are additional components as compared with the normal and LINER galaxies. In NGC7743, the old metal-rich and 1-Gyr components are still dominant, contributing ≈40 per cent each to the flux at λ5780 Å throughout in the inner ≈1 kpc. At the nucleus, the remaining ≈20 per cent of the flux is a result of a 100-Myr-old component. Outside the nucleus, the remaining flux (up to ≈15 per cent) seems to be the result of an old metal-poor component. The components younger than 100 Myr and FC do not appear to contribute significantly. Finally, the reddening $E(B-V)_i \approx 0.14$ at the nucleus, decreases to ≈0.02 at 1 kpc.

At the nucleus of ESO138-G1 the components with 100 Myr and

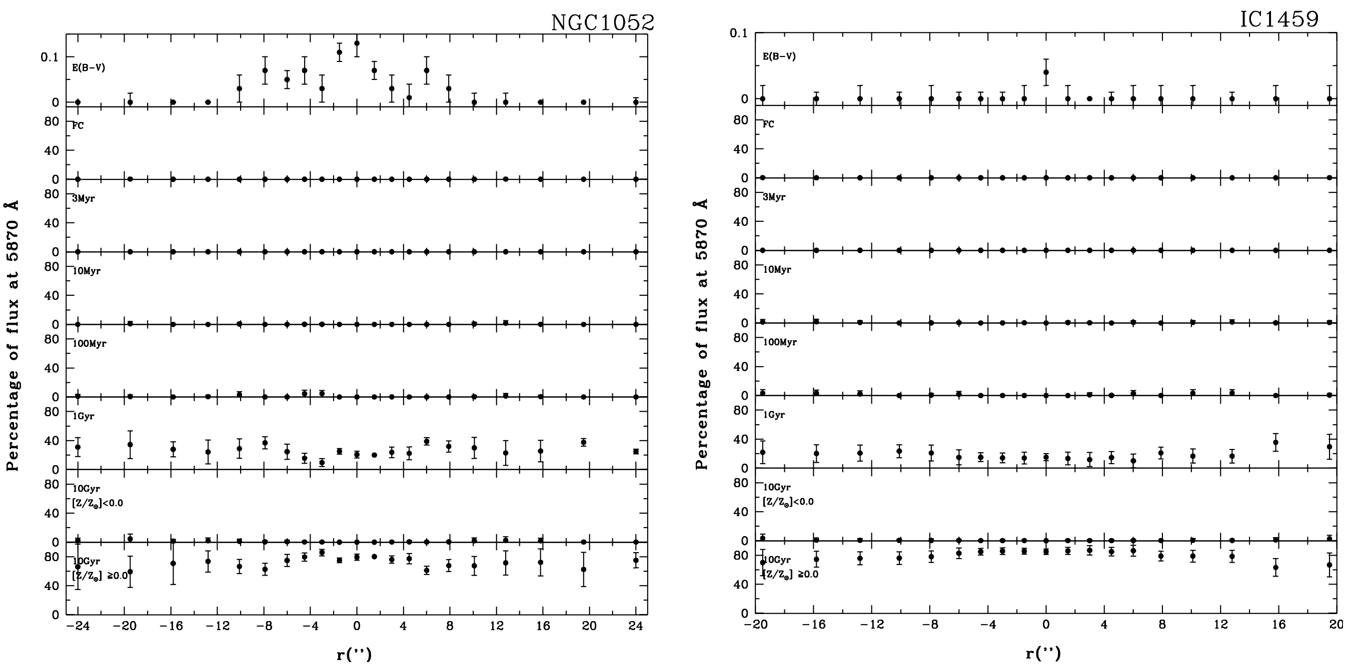

Figure 10. LINERs: as in Fig. 9.

1 Gyr are dominant, contributing respectively 35 and 50 per cent of the flux at λ5870 Å and falling abruptly outside the nucleus. The stellar population outside the nucleus (distance $\gtrsim$1 kpc) is similar to those of normal and LINER galaxies. The components younger than 100 Myr and the FC do not contribute significantly. At the nucleus, there seems to be an old metal-poor component contributing $\approx$20 per cent of the flux. However, because of the degeneracy problem discussed earlier, this component could be the result of an FC. The reddening is $E(B-V)_i \approx 0.05$ at the nucleus and decreases to $\approx$0.00 at 1 kpc.

At the nucleus of Mrk463E the dominant components are those of ages 100 and 3 Myr, contributing 40 and 20 per cent of the flux at λ5870 Å, respectively. The remaining flux is distributed among the FC (10 per cent), 1-Gyr (15 per cent) and old rich (15 per cent) components. Outside the nuclear region (>2 kpc), the contributions of the 100- and 3-Myr components decrease and the stellar population is dominated by the 1-Gyr plus 100-Myr components on one side and 1-Gyr plus 10-Gyr components on the other side of the nucleus. The reddening is $E(B-V)_i = 0.14$ at the nucleus, decreasing to $\approx$0.00 at $\approx$2 kpc.

In Figs 12–15 we compare the nuclear observed spectrum (solid line) with the synthetic one (dashed line) for the normal galaxy NGC6684, the LINER IC1459 and the Seyferts NGC7743 and ESO138-G1. The synthetic spectra were constructed using the star cluster templates (Bica & Alloin 1986a, 1987) combined in the proportions given by the synthesis. Signature of the presence of

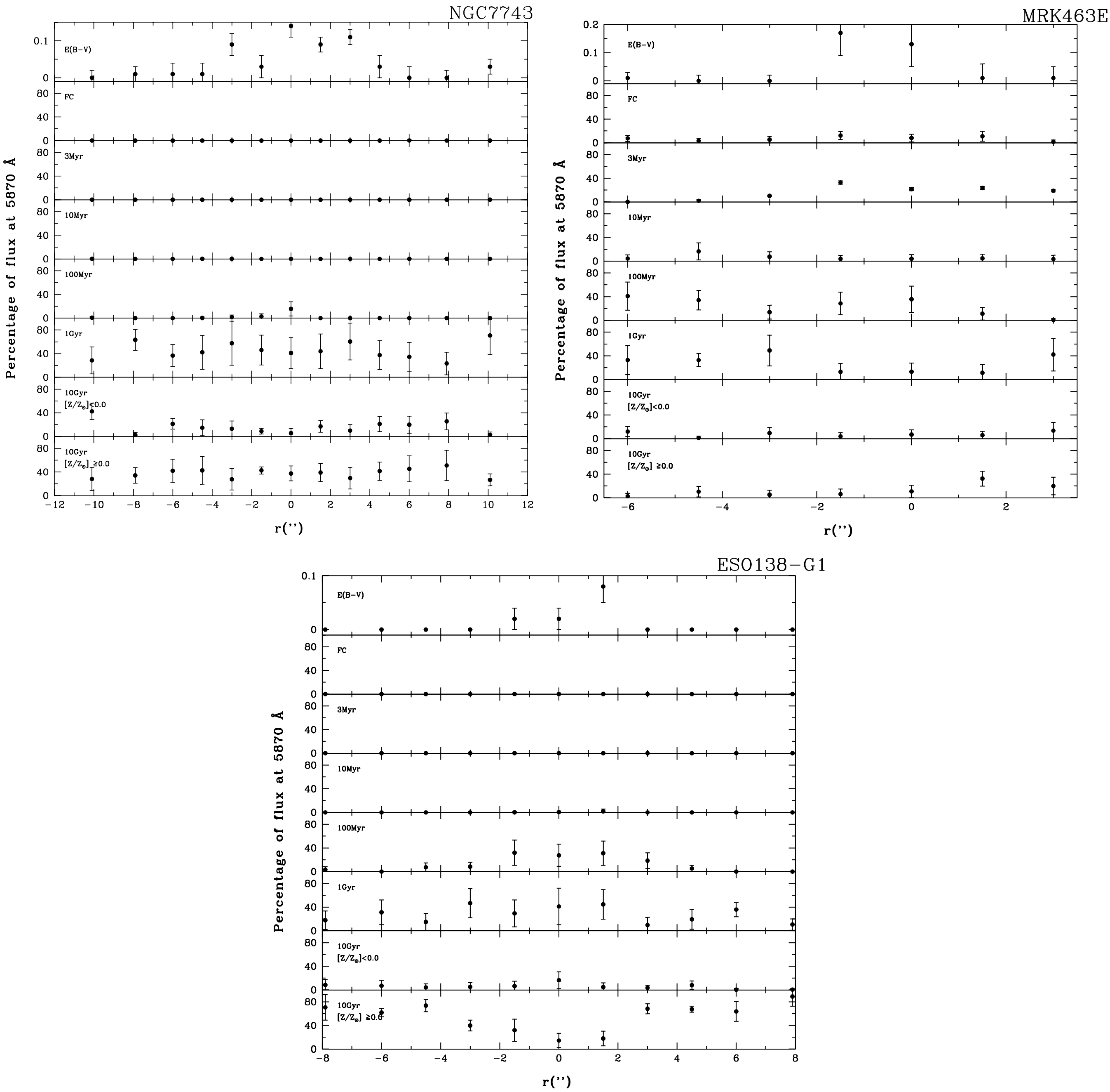

Figure 11. Seyferts: as in Fig. 9.

intermediate-to-young stars such as the high-order Balmer lines in absorption (e.g. H8, H9, H10), as observed by Storchi-Bergmann et al. (2000) and González Delgado et al. (2000), are easily observed in NGC7743 (Fig. 14), confirming the results of the synthesis. Nevertheless, these signatures could not be observed in the cases of ESO138-G1 (Fig. 15) and Mrk463E. We interpret this lack of detection as a result of the large Ws of the emission lines, which completely fill the underlying absorptions. The insert in Fig. 15 shows the pure nuclear emission spectrum of ESO138-G1 after the subtraction of the synthesized stellar population in the region of the high-order Balmer lines. The resulting Balmer decrements of the emission lines are consistent with those expected in recombination theory, suggesting that the synthesized stellar population is correct. In addition, the emission-line ratios involving the forbidden lines also suggest some contribution of photoionization by young stars, as they locate these two nuclei in the borderline between the H II region and Seyfert 2 loci in diagnostic diagrams.

6 SUMMARY AND CONCLUSIONS

We have investigated the behaviour of a number of stellar absorption features and continuum colours as a function of distance from the nucleus for eight E-S0 galaxies – three normals, two LINERs and three Seyfert 2s – in order to make a comparative study.

The run of the equivalent widths and colours as a function of distance from the nucleus for the LINERs is similar to that of the normal galaxies, both having a nucleus redder than the surroundings and nuclear absorption lines stronger than outside the nucleus. The nuclear Ws in the blue (W_{H9}, $W_{Ca\,II K}$, $W_{G\text{-band}}$ and $W_{CN\text{-band}}$) are 10–20 per cent smaller than the average value for the normal galaxies.

Two Seyfert 2 galaxies studied here present bluer F_{5870}/F_{4020} nuclear colours than the surroundings and nuclear absorption lines weaker than extranuclear ones, corresponding to dilution by a blue continuum of ≈60–80 per cent. In the three cases, the nuclear Ws values are smaller than those of the normal galaxies, while outside the nucleus, only Mrk463E shows significantly smaller values (>30 per cent) than the extranuclear values of the normal galaxies.

A more significant result for the Seyferts is obtained by combining our results with those for the nine S0 Seyfert 2 galaxies from the larger sample of Cid Fernandes et al. (1998). In 10 out of 12 S0 Seyfert 2s (≈80 per cent), the nuclear Ws are smaller than those of normal S0 galaxies, suggesting dilution by a blue continuum, while at ≈1 kpc from the nucleus, 4 out of 12 (≈30 per cent) still present significant (>30 per cent) dilution in the blue Ws when compared with those of normal galaxies.

We have subsequently performed spectral synthesis as a function of distance from the nucleus, using a base of 12 spectral elements representing stellar populations of different ages and metallicities plus a power law representing a featureless continuum. We have introduced two additional spectral features in the blue in order to better constrain the synthesis, and present the calibration of the Ws of these features in terms of age and metallicity. We have tested the robustness of the solutions obtained from the synthesis using simulated composite spectra and have concluded that it discriminates well between the different age components, but not between different metallicities in the 10- and 100-Myr age bins. For signal-to-noise ratios ≤10 we find also that there is a degeneracy between FC, the 10-Myr and low-metallicity 1- and 10-Gyr components. The use of near-IR Ca II triplet and UV metal lines could avoid this degeneracy (Bica & Alloin 1987; Bica 1988; Bonatto et al. 1998). For example, Ca II triplet does not suffer from dillution by young components, while Ca II K does (Bica & Alloin 1987). Together they are sensitive both to age and metallicity. Ideally, in the synthesis, a spectral range as wide as possible should

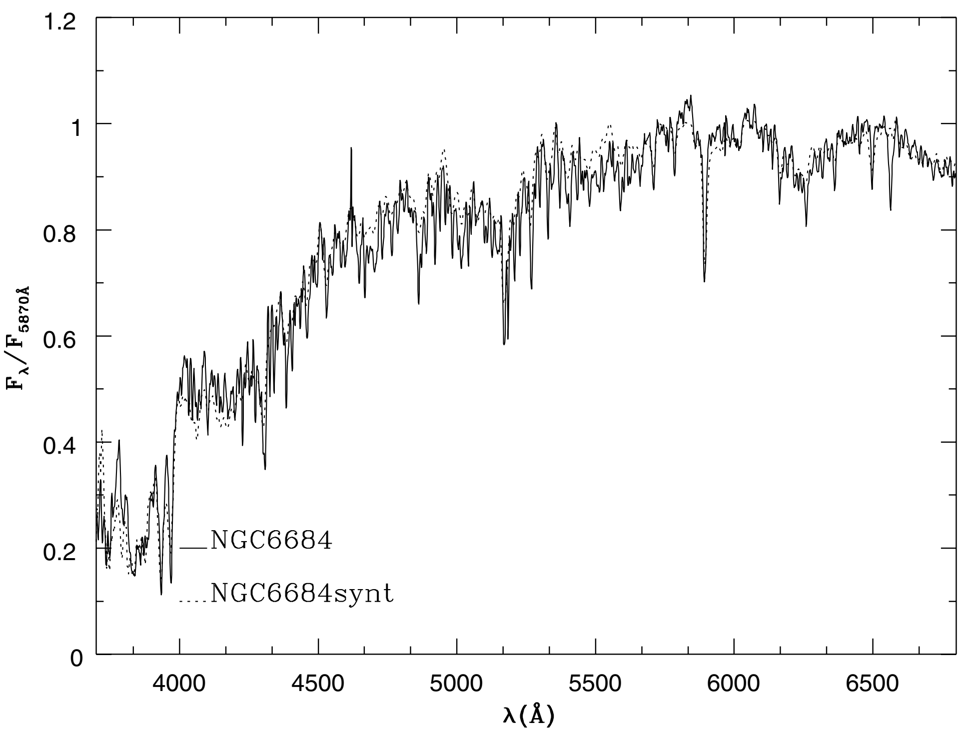

Figure 12. Observed nuclear and synthetic spectra of the normal galaxy NGC6684. The nuclear spectrum was smoothed to match the lower resolution of the synthetic spectrum.

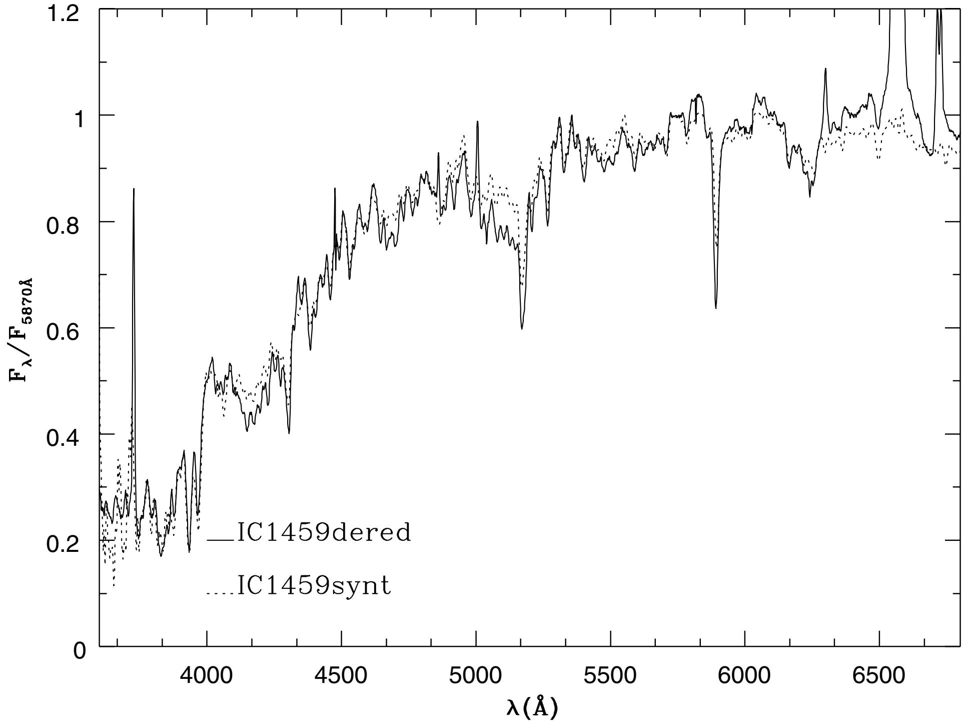

Figure 13. Observed nuclear and synthetic spectra of the IC1459 galaxy. The nuclear spectrum was smoothed to match the lower resolution of the synthetic spectrum.

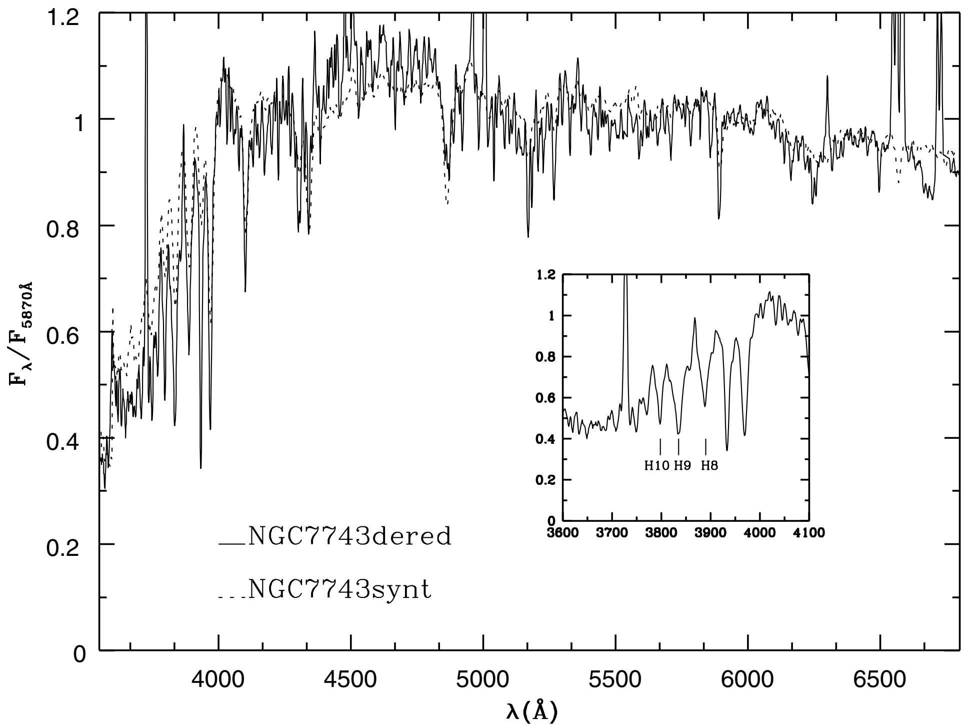

Figure 14. Observed nuclear and synthetic spectra of the NGC7743 galaxy. The nuclear spectrum was smoothed to match the lower resolution of the synthetic spectrum. Insert: the near-UV region with the high-order Balmer lines in absorption.

be used (e.g., from UV to IR) in order to include features sensitive to all relevant parameters.

In the normal galaxies the stellar population – obtained from the synthesis – is dominated by the old metal-rich component at the nucleus, with its contribution decreasing outwards, while the contribution of the 1-Gyr-old component increases outwards.

For the LINERs, the only difference relative to normal galaxies is that they have ≈10–20 per cent larger contribution of the 1-Gyr component at the nucleus. We found no signature of the young massive stars found by Maoz et al. (1998) in four out of seven LINERs with a compact nuclear UV source (which comprise about 25 per cent of the LINERs).

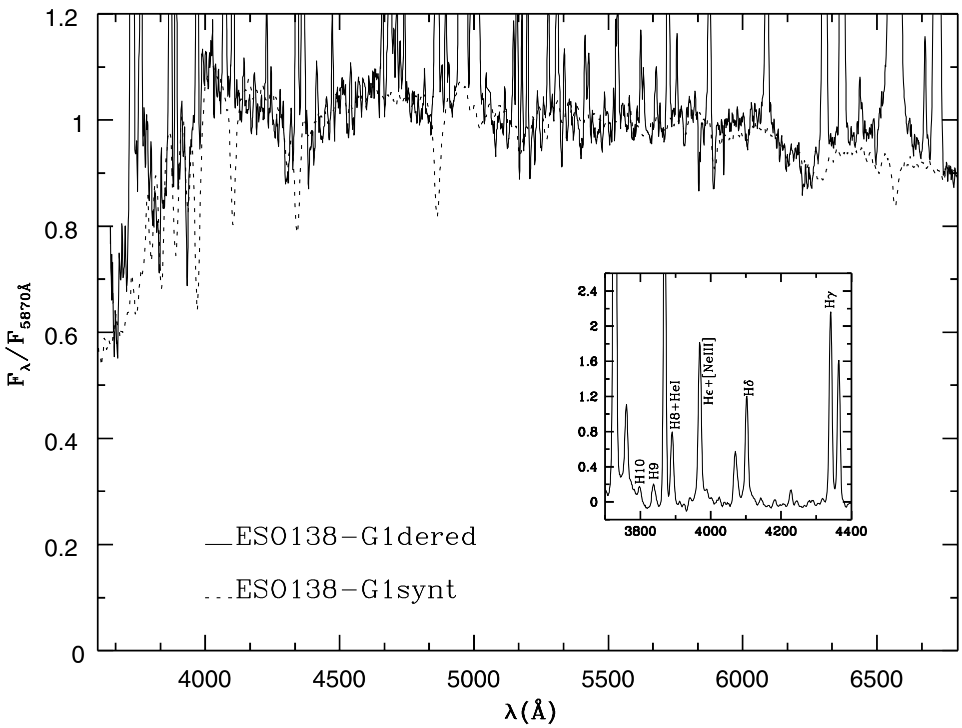

Figure 15. Observed nuclear and synthetic spectra of the ESO138-G1 galaxy. The nuclear spectrum was smoothed to match the lower resolution of the synthetic spectrum. Insert: the near-UV region after subtraction of the stellar population, showing the high-order Balmer lines in emission.

In the Seyfert 2s, the synthesis gives additional components: at the nucleus in all three cases, there is a significant (20–40 per cent of the flux at λ5870 Å) contribution of a 100-Myr-old component. This result is similar to that found by Schmitt et al. (1999) in the synthesis of the nuclear spectra of 20 Seyfert 2 galaxies. At the nucleus of Mrk463E there is also the contribution of the 3-Myr age component and of an FC. In ESO138-G1, the 20 per cent contribution of the old metal-poor component is most probably the result of an FC (because of the degeneracy problem discussed above).

Outside the nucleus, the stellar population of ESO138-G1 is similar to that of normal galaxies, while in Mrk463E the contribution of the old metal-rich component is very small (<20 per cent). In the case of NGC7743, the ≈20 per cent contribution of the old metal-poor component is not observed in normal galaxies. There are two possibilites for its origin: (i) an excess of old stars of low metallicity or (ii) because of its possible degeneracy with FC, this component is the result of an extended FC which could be scattered nuclear light, as observed on near-UV images of some Seyfert 2 galaxies (e.g. NGC1068, Mrk3 and Mrk573: Pogge & De Roberts 1993).

The nuclear internal reddening derived from the synthesis is very small in the case of the normal galaxies [$E(B-V)_i \approx 0.00$], reaches $E(B-V)_i \approx 0.10$ for the LINERs and $E(B-V)_i \approx 0.15$ for the Seyfert 2 galaxies. Outside the nucleus essentially no internal reddening was detected.

ACKNOWLEDGMENTS

DR, TSB and EB acknowledge support from the Brazilian Institutions CNPq, CAPES and FAPERGS. We thank the referee Dr. Rosa M. González Delgado for valuable suggestions which helped to improve the paper.

The NASA/IPAC Extragalactic Database (NED) is operated by the Jet Propulsion Laboratory, California Institute of Technology, under contract with the National Aeronautics and Space Administration.

REFERENCES

Aretxaga I., Terlevich E., Terlevich R. J., Cotter G., Díaz Á. I., 2001, MNRAS, in press
Bica E., 1988, A&A, 195, 76
Bica E., Alloin D., 1986a, A&A, 162, 21
Bica E., Alloin D., 1986b, A&AS, 66, 171
Bica E., Alloin D., 1987, A&A, 186, 49
Bica E., Alloin D., Schmitt H. R., 1994, A&A, 283, 805 (BAS94)
Bonatto C. J., Bica E., Alloin D., 1989, A&A, 226, 23
Bonatto C., Pastoriza M., Alloin D., Bica E., 1998, A&A, 334, 439
Burstein D., Heiles C., 1982, AJ, 87, 1165
Cid Fernandes R., Jr, Storchi-Bergmann T., Schmitt H. R., 1998, MNRAS, 297–579
González Delgado R., Heckman T. M., Leitherer C., Meurer G. R., Krolik J., Wilson A. S., Kinney A., Koratkar A., 1998, ApJ, 505, 174
González Delgado R., Leitherer C., Heckman T. M., 1999, ApJS, 125, 489
González Delgado R., Heckman T. M., Leitherer C., 2000, ApJ, in press
Heckman T. M., González Delgado R., Leitherer C., Meurer G. R., Krolik J., Kinney A., Koratkar A., Wilson A. S., 1997, ApJ, 482, 114
Keel W. C., 1983, ApJ, 269, 466
Koski A. T., 1978, ApJ, 223, 56
Maoz D., Koratkar A., Shields J. C., Ho L. C., Filippenko A. V., Sternberg A., 1998, AJ, 116, 55
Pogge R. W., De Robertis M. M., 1993, ApJ, 404, 563
Schlegel D. J., Finkbeiner D. P., Davis M., 1998, ApJ, 500, 525
Schmitt H. R., Bica E., Pastoriza M. G., 1996, MNRAS, 278, 965
Schmitt H. R., Storchi-Bergmann T., Cid Fernandes R., 1999, MNRAS, 303, 173
Storchi-Bergmann T., Bica E., Pastoriza M. G., 1990, MNRAS, 245, 749
Storchi-Bergmann T., Cid Fernandes R., Schmitt H. R., 1998, ApJ, 501, 94
Storchi-Bergmann T., Raimann D., Bica E., Fraquelli H., 2000, ApJ, 544, 747

This paper has been typeset from a TEX/LATEX file prepared by the author.